## Title

The study on the effect of anti-VEGF antibody on apparent permeability of a human breast cancer model using macromolecular contrast media-enhanced magnetic resonance



## Author

Pham, Christine,

## Publication Date

1996

Peer reviewed|Thesis/dissertation

# The Study on the Effect of Anti-VEGF Antibody on Apparent Permeability of a Human Breast Cancer Model Using Macromolecular Contrast Media-Enhanced Magnetic Resonance Imaging

by

Christine Pham

A Thesis

Submitted in partial satisfaction of the
requirements for the M.D. with Thesis Program
of the
University of California, San Francisco

## TABLE OF CONTENTS

## ABSTRACT

Magnetic resonance imaging (MRI) enhanced with a macromolecular contrast medium (MMCM) has been shown previously to permit estimation of tumor microvascular permeability which correlates closely with histologic microvascular density, an established surrogate of tumor angiogenesis. A refined MMCM-enhanced MRI technique used in combination with tumor volume measurements was applied to monitor the potential effects of anti-vascular endothelial growth factor (VEGF) antibody on tumor microvascular characteristics and growth. Human breast carcinoma (MDA-MB-435) cells were xenografted in athymic rats. Beginning one week after tumor cell implantation, anti-VEGF and a control antibody (1 mg doses) were administered at 3-day intervals for a total of three dosages. Tumor dimensions were monitored daily. Tumors were imaged following administration of albumin-(Gd-DTPA)$_{30}$ using a heavily T1-weighted 3D-SPGR pulse sequence prior to animal sacrifice. Changes in tumor and blood longitudinal relaxivity, $\Delta R1$, were analyzed using a bi-directional two-compartment kinetic model to estimate tumor fractional blood volume (BV) and permeability surface area product (PS). Data showed significant reductions ($p < 0.05$) in tumor growth rates and in MRI-assayed PS. No significant change was observed in tumor fractional blood volume. Results reconfirmed in a new tumor model that anti-VEGF antibody suppresses tumor growth. MRI data analysis demonstrated that anti-VEGF antibody was associated with a reduction of tumor microvascular permeability to a macromolecular probe and this reduction could be detected and quantified by MMCM-enhanced MRI.

# INTRODUCTION

Magnetic resonance imaging (MRI) enhanced with macromolecular contrast medium (MMCM) has the potential to measure physiological and anatomical characteristics of tumor vasculature and to monitor the effects of drugs intended to alter vascular characteristics (1,2). An essential and upregulated element of tumor vasculature is the process of angiogenesis.

Angiogenesis is a fundamental process in both normal and diseased tissues. It is essential for embryogenesis, corpus luteum formation, and wound healing (3). Angiogenesis, however, is also essential for the rapid growth and metastasis of solid tumors (3-5). With the development of new strategies and drugs to interrupt or otherwise modify the angiogenesis process, understanding angiogenesis has become a subject of intense investigation.

Neovascularization is necessary for the growth of solid tumors beyond 2-3 mm in diameter (3,6). In addition, the potential of a tumor to successfully metastasize can be linked to angiogenesis, neovasculature being required at both the beginning and the end of the metastatic cascade. More angiogenic primary tumors possess a greater number and size of microvessels through which metastasizing cells are shed into the blood stream; with increased angiogenesis the number of metastasizing cells can increase 100-fold or more (7). The well-recognized hyperpermeability of tumor vessels, related to angiogenesis, may also contribute to the transendothelial escape of tumor cells (8). Having entered the circulation, the cells must survive the circulation, escape immune surveillance, penetrate the endothelium of the target organ, and again induce angiogenesis in order to grow beyond 2 mm in diameter. Angiogenesis may not be solely responsible for metastases; however, the inhibition of angiogenesis prevents the

growth of tumor cells at both the primary and secondary sites and thereby can prevent the emergence of metastases (5, 9).

Being a limiting factor for both tumor growth and metastases, angiogenesis has been assumed to correlate with tumor aggressiveness. This assumption has been supported in clinical series investigating a variety of tumor types. Histologic assessments of angiogenesis based on microvascular density (MVD), the number of endothelial clusters in a high-power microscopic field, has been shown to be an independent prognostic indicator of metastatic potential and disease-free survival in patients with primary breast cancer (10,11). The adverse prognostic significance of high histologic MVD has been demonstrated in a spectrum of malignancies and is accepted as a measurable surrogate of angiogenesis (11).

Angiogenesis is a complex process with a combination of both stimulators and inhibitors. Stimulators, or angiogenic factors, are secreted by neoplastic cells and tumor-associated inflammatory cells. These factors act in a paracrine fashion to increase the production of endothelial cells and to prepare the local environment for the ingrowth of new vascular buds. Subsequently, affected endothelial cells in juxta-tumoral blood vessels divide rapidly, whereas those in normal tissues do not (4).

Tumor-secreted vascular endothelial growth factor (VEGF) has been suggested to affect angiogenesis directly and indirectly by its multiple functions. In vitro and in vivo studies have supported the role of VEGF as an endothelial cell-specific mitogen and thus this small protein affects tumor growth. VEGF strongly stimulates the proliferation and migration of endothelial cells in culture and induces neovascularization in rabbit cornea and chick chorioallantoic membrane assays (12). Non-VEGF secreting tumorigenic cell lines transfected with human VEGF cDNA and implanted into nude mice showed higher angiogenic activity and increased tumor growth (13). The systemic administration of anti-VEGF

monoclonal antibody (antibody) in tumor-bearing mice markedly inhibited the growth of subcutaneous xenografts and reduced metastases and tumor vascularity (9). Although undoubtedly affecting endothelial cells, neither VEGF nor its antibody have any effect on the growth rate of the tumor cells in vitro (9, 12,14).

VEGF is also known as vascular permeability factor (VPF) by virtue of its potent vascular permeability enhancing effects. In low nanomolar to picomolar concentrations, VEGF/VPF increases the permeability of venules and small veins to plasma proteins with a potency approximating 50,000 times that of histamine on a molar basis (15,16). VEGF/VPF is thought to be responsible for the enhanced permeability of tumor blood vessels with respect to macromolecular solutes and the exudative fluid accumulation associated with ascites tumors (15, 17). VEGF/VPF protein staining in guinea pig solid tumors was concentrated in tumor blood vessels, initially evident in preexisting venules and small veins and later in newly induced tumor microvessels; these VEGF-stained vessels were also shown to be hyperpermeable to macromolecules (10). Acting similarly to its inhibitory action on tumor growth, function-neutralizing monoclonal antibody to VEGF/VPF has been shown to completely inhibit VEGF/VPF-mediated enhanced vascular permeability as measured by the Miles assay(6,14). Hypothetically, the secretion of VEGF from tumor cells induces hyperpermeability of nearby microvessels, leading to the extravasation of proteinaceous fluid into the paratumoral interstitium. This exudate provides an ideal matrix for the ingrowth of new capillaries (6.19). Thus, VEGF appears to be involved, at least partially, in an early stage of the angiogenesis cascade. The VEGF-induced hyperpermeability to macromolecules provides a window of opportunity for an imaging assay of the angiogenesis process.

To date, there is no single or direct measure of angiogenesis. Currently quantitative surrogates of tumor angiogenesis include tumor growth rate and histological microvessel density (MVD) (10,11). Although microscopic counting of capillaries on specially stained tumor specimens has been a useful indicator of angiogenesis, MVD is not a gold standard of angiogenesis nor is it an ideal clinical tool. Being invasive, by definition, serial MVD assays necessary to monitor progress of therapy are not practical. MVD is also subject to sampling errors because tumors are notoriously heterogeneous and the entire tumor cannot be examined.

An imaging assay for angiogenic activity would be clinically powerful, particularly if the method were quantitative, non-invasive, could sample the entire tumor, and could be repeated at frequent intervals. In a qualitative way, radiologists have been imaging tumor microvasculature, often termed as "vascularity" and on the "capillary phase" of angiograms. The general hypervascularity of cancers may be largely responsible for the reported high sensitivity of Gd-enhanced MRI for the detection of breast cancers. The dense microvascular network of cancers leads to a higher tumor accumulation of even small molecular contrast medium than is observed in normal breast tissue (20,21). However, the small-molecular contrast media now in clinical use rapidly diffuse through the endothelial barriers of both normal and tumoral vessels (22,23). Macromolecular contrast media (MMCM) have molecular dimensions that approximate those of serum albumin and thus are well-suited to define the high density and hyperpermeability inherent to tumor microvasculature. MMCM diffuse very slowly, if at all, through normal endothelial barriers (22-24). MMCM can be used advantageously for angiography as these large paramagnetic probes recirculate in the blood for an hour or longer and can be used to generate quantitative measurements of blood volume and apparent

permeability, expressed as the permeability surface area product (PS) (24-26). The accumulation of a $T_1$-shortening contrast medium generally causes a local increase in MR signal intensity. Initially after intravenous administration, the MMCM is confined to the intravascular space and thus the signal enhancement relates to the tumor fractional blood volume. Over time, MMCM moves across the endothelium of capillaries, accumulating in the interstitium and progressively increasing enhancement. The rate of increased enhancement relates to the rate of leak, *i.e.* the capillary permeability (25,26).

The current study was undertaken to determine if MRI enhanced with MMCM could identify and measure the effect of an anti-angiogenesis intervention on microvascular characteristics. Specifically, we hypothesized that anti-VEGF antibody treatment may lead to a suppression of tumor microvessels permeability or vascularity, as reflected in MRI-derived PS and BV values, and corroborated by suppression of tumor growth.

## MATERIALS AND METHODS

### Animal and Tumor Model

The study was conducted with the approval of the institutional Committee for Animal Research conforming to the guidelines of the National Institutes of Health for the care and use of laboratory animals. The human breast cancer cell line MDA-MB-435, generously provided by Dr. Robert Stern (Department of Pathology, University of California, San Francisco), was cultured under conditions previously described (27). This cell line is an estrogen-receptor negative, poorly differentiated adenocarcinoma that expresses VEGF (personal communication: O Melnyk, Department of Medicine, University of California-San Francisco) and has been shown to be tumorigenic in nude mice (27). Approximately $5x10^6$ tumor cells suspended in a total volume of 0.3 ml (1 part sterile saline: 1 part Matrigel®) were injected with a 25-gauge needle in the mammary fat pads of 12 four-week-old female homozygous athymic rats (Harlan, Indianapolis, IN).

### Antibody Treatment

One week after tumor cell inoculation, when the tumors were typically 5 mm in diameter, six randomly chosen animals were given anti-VEGF antibody (a $VEGF_{165}$, $IgG_1$ isotype) and the other six received a control antibody directed against the cell surface protein gp120 (anti-gp120). Antibody synthesis has been described previously in detail (14). For each animal, a dose of 1 mg of antibody (anti-VEGF or anti-gp120) in a total volume of 0.3 ml of sterile saline solution was injected intraperitoneally (i.p.) every third day, for a total of three doses. The dose of antibody, on a per weight basis, was chosen to equal the dose previously used in anti-VEGF antibody studies with mice (9,12). Anti-gp120, a control antibody matched to anti-VEGF isotype, was used to ensure that any difference

in the parameters measured between the index and control treated tumors was not attributable to a nonspecific action of immunoglobulin administration.

**Tumor growth and size**

The growth curves of anti-VEGF- and anti-gp120 antibody treated tumors were determined by daily caliper measurements. Tumor volume was calculated from two-dimensional measurements, assuming an ellipsoidal shape (28). Logarithmic transformation was conducted for tumor volumes, and the log transformed values fitted to a linear fit to obtain the slope, or the measurement of growth rate. Immediately after MR imaging, animals were sacrificed and the tumors excised and weighed.

**MRI**

MRI was performed on an Omega CSI-II system operating at 2 Tesla (Bruker Instruments, Fremont, CA) and equipped with Acustar S-150 self-shielded gradient coils (±20 Gauss/cm, 15 cm inner diameter). Animals were anesthetized with pentobarbital (50 mg/kg, i.p.) and a 23-gauge butterfly needle (Abbott Laboratories, North Chicago, IL) was inserted into the tail vein for intravenous injection of contrast medium. A three-dimensional (3D-) spoiled gradient-refocused acquisition in a steady state (SPGR) pulse sequence (TR/TE= 50ms/1.4 ms; 128 x 128 x 16 matrix; 50 x 50 x48 mm field of view) was used to monitor the change in signal intensities in venous blood (inferior vena cava) and tumor tissue resulting from contrast enhancement. The total acquisition time per matrix was 1'42", thus allowing adequate temporal resolution for kinetic analysis. Precontrast longitudinal relaxation time ($T_1$) estimates for blood and tissue were obtained by curve fittings based on a set of similar 3D-SPGR sequences with TR times varying from 50 ms to 2000 ms (29). Albumin-(Gd-DTPA)$_{30}$, a prototype intravascular macromolecular contrast medium for MRI, was administered intravenously (0.03 mmol Gd/kg body weight). Albumin-(Gd-DTPA)$_{30}$ has a

molecular weight of approximately 92 kDA, a plasma half-life of 3.5 hours, and produces prolonged enhancement of the blood pool (23,30). Dynamic 3D-SPGR was continued for 60 minutes after an intravenous bolus injection of MMCM to permit estimation of microvascular parameters, specifically fractional blood volume (BV) and permeability surface area product (PS) (10). Anatomical coverage included the tumor, liver, and inferior vena cava (IVC). In addition, a mineral oil phantom was placed in the field of view to permit correction for minor spectrometer variations. The animals were sacrificed by pentobarbital overdose and thoracotomies immediately after the MRI protocol.

**MRI data analysis**

Signal intensity values were obtained for every time point from the tumor rim, tumor center, from IVC blood, and from the oil phantom. Tumor rim and center regions-of-interest (ROI's) were anatomically defined in the pre-contrast images. Tumor rim was recognized as the most outer layer of approximately 10 pixels from the tumor periphery; tumor center was identified as the region of the tumor which was approximately 15 pixels from the periphery of the tumor. Four to six ROI's (a minimum of 30 pixels/region), which in total encompassed a minimum of 50% of the tissue, were analyzed over two to three contiguous anatomical image slice using an image analysis program (MR Vision, Menlo Park, CA). The signal responses from various tumor regions and the IVC blood were corrected for potential temporal spectrometer variation by normalizing to the phantom. Precontrast relaxation rate, $R_1$ (= $1/T_1$), estimates for blood and tumor were obtained by curve fittings based on five 3D-SPGR sets obtained precontrast with TR's (time to repeat) varying from 50 ms to 2000 ms to an equation describing the innate (i.e. no contrast) proton relaxation response curve of tissue or blood. Postcontrast $R_1$ values can be calculated based on signal intensity and knowledge of precontrast values (29). The precontrast $R_1$ for each

response was subtracted from the postcontrast $R_1$ to obtain the change in the relaxation rate, $\Delta R_1$, at all postcontrast time points. $\Delta R_1$ is assumed to be directly proportional to the local gadolinium concentration [Gd] in a tissue (31)

**Kinetic Analysis**

The $\Delta R_1$ data were submitted to kinetic analysis for estimation of fractional plasma volume (fPV) and measures of capillary permeability, specifically fractional leak rate (FLR); fractional reflux rate (FRR); and permeability surface area product (PS). The model used to analyze the $\Delta R_1$ data obtained from blood and tumor is shown in **Figure 1.**

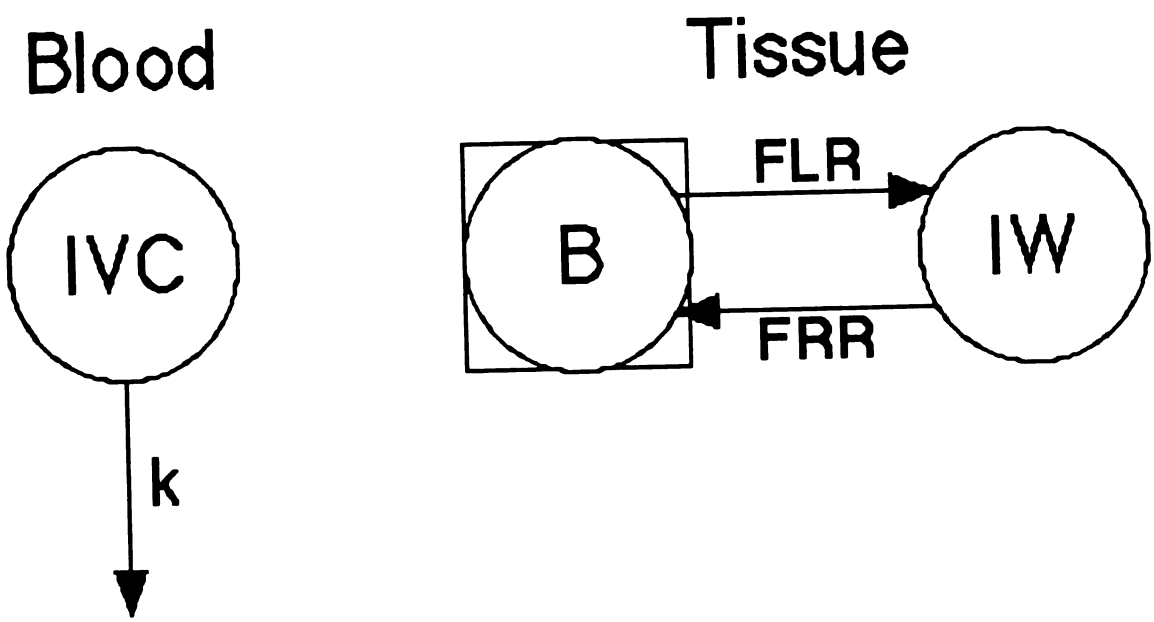


Fig. 1 Diagram of linear, bi-directional two-compartment model. The kinetics of Gd disappearance from the blood following bolus intravenous injection of albumin-$(Gd\text{-}DTPA)_{30}$ can be described by a single compartment (IVC) with fractional turnover rate of k ($m^{-1}$) and initial condition IC (not shown). The

tumor or tissue model is made up of two compartments, tissue blood (B) and tissue interstitial water (IW). This model describes the kinetics of fractional transport of albumin-(Gd-DTPA)$_{30}$ from B to IW, designated FLR for fractional leak rate ($m^{-1}$), and from IW to B, designated FRR for fractional reflux rate ($m^{-1}$). The blood compartment of the tissue is shown as a circle inside of a box signifying that the response in this compartment is a forcing function characterized by the response in the IVC multiplied by a proportionality constant, the fractional blood volume (fBV) of the tissue.

Thus the five parameters of the model (k, IC, FLR, FRR and fBV) are fitted to the $\Delta R_1$ data from the IVC, $\Delta R_{1,V}(t)$, and from the tumor, $\Delta R_{1,T}(t)$, using the SAAM II program (SAAM Institute, Seattle, Washington) which employs standard variance-weighted non-linear regression. The uncertainty estimates of the model parameters and measures of the model parameters are determined from the covariance matrix at the least-squares fit.

The estimation of the permeability-surface area product, PS, (ml $hr^{-1}$ $cm^{-3}$ of tissue) of the tissue to albumin-(Gd-DTPA)$_{30}$ from the model parameters has been discussed in detail previously (24). Briefly, PS can be calculated as the product of fBV and FLR, once fBV is corrected for hematocrit, to yield an estimate of the plasma volume of the tissue, and the magnitude of FLR is multiplied by 60 to convert to hours. This calculation is based on an approximation of the Renkin-Crone model of capillary permeability (32,33) where it is assumed that the blood flow rate through the tissue is large as compared to PS, a reasonable assumption for a macromolecule such as albumin-(Gd-DTPA)$_{30}$. It is also assumed that the central venous hematocrit (used to convert tissue blood volume to tissue plasma volume) is a good approximation of tissue blood hematocrit.

All values were expressed as mean ± S.D. The Mann-Whitney U Test (Abacus Concepts Inc., Berkeley, CA) was conducted to compare the differences in the BV, FLR, and PS measurements between anti-VEGF and control-treated tumors. This nonparametric test does not assume that the data analyzed come from a normal distribution. Furthermore, since the Mann-Whitney test does not look at the observations but instead considers their ranks, it is resistant to outliers in either of the two groups being compared; given the size of the study, outliers may skew the means of each of the two groups of tumors studied. An unpaired, two-tail t-test was employed to compare the differences betwen tumor growth rate and weight between anti-gp120 and anti-VEGF antibody treated tumors. In both the Mann-Whitney U test and t-test, a probability of less than 0.05 was considered statistically significant.

## RESULTS

### Effect of anti-VEGF Antibody on Tumor Growth and Weight

A significant reduction ($p = 0.006$) in tumor growth rate, determined by linear regression of logarithmically transformed tumor volumes, was observed in animals treated with anti-VEGF antibody as compared to those treated with anti-gp120 antibody ($0.11 \pm .001$ $cm^3$ $day^{-1}$ vs. $0.20 \pm .027$ $cm^3$ $day^{-1}$, respectively). See **Figure 2.** The anti-VEGF growth rate inhibition corresponded to a 58% decrease in mean tumor weight at the time of animal sacrifice. The weights of anti-VEGF and anti-gp120 treated tumors were $1.1 \pm 0.3$ g and $2.6 \pm 0.8$ g, respectively ($p = 0.005$).

### Effect of Anti-VEGF Antibody on MRI-Assessed Microvascular Characteristics

Representative axial MR images of tumor-bearing animals administered either anti-gp120 antibody (control) or anti-VEGF antibody before contrast medium administration, one minute, and sixty minutes postcontrast are shown in **Figure 3.** The figure also includes two pixel maps of PS values calculated for each image element (pixel) with higher PS values assigned a lighter shade of gray. As observed consistently for all animals, these images show a smaller tumor size for the anti-VEGF antibody treated animal. The images also show an obvious enhancement in the liver, blood vessels, and the tumor. The calculated pixel-by-pixel PS map included in Figure 3 indicates a lower microvascular permeability (less intensity) in the anti-VEGF treated animal.

Mean enhancement responses ($\Delta R_1$) for IVC blood and tumors for all animals over the 60-minute imaging period are shown in **Figure 4.** Data show a significantly higher rate of contrast enhancement (increased slope) in the control treated tumors compared to the anti-VEGF antibody treated group ($p = 0.01$). However, enhancement is temporally increasing in both tumor groups relative to

venous blood enhancement, relationships reflecting transendothelial diffusion of macromolecular contrast medium from the blood into the tumor extravascular space.

The two-compartment, bi-directional model of capillary permeability fit the date well for each of the 12 studies. The model parameters for each study are shown in **Table 1**. FLR and FRR values were significantly reduced in the anti-VEGF group as compared to the control-treated group when analyzed for the whole tumor and tumor rim, but not for tumor center. Calculated PS values were significantly reduced in the whole tumor ($p = 0.011$), in the tumor rims ( $p = 0.0037$), and the tumor centers ($p = 0.031$) in the anti-VEGF antibody treated animals as compared to the anti-gp120 antibody treated animals (see **Figure 5**). As compared to the control-treated group, the minor trend for lower BV ($ml \bullet cm^{-3}$) in the anti-VEGF antibody treated tumor rim ($5.1 \pm 1.5\%$ vs. $6.0 \pm 2.4\%$, $p = 0.14$) and tumor center ($1.6 \pm 0.7\%$ vs. $2.2 \pm 0.8\%$, $p = 0.63$) was not statistically significant.

**Fig. 2** Effects of anti-VEGF antibody on the growth of MDA-MB-435 tumors. Tumor volumes of the anti-VEGF antibody (○ ) and anti-gp120 antibody (■ ) treated groups are expressed as mean ± SD (n=6 in each antibody group). Error bars represent SD. Antibody was administered on days 8, 11, and 14 post-tumor cell inoculation.

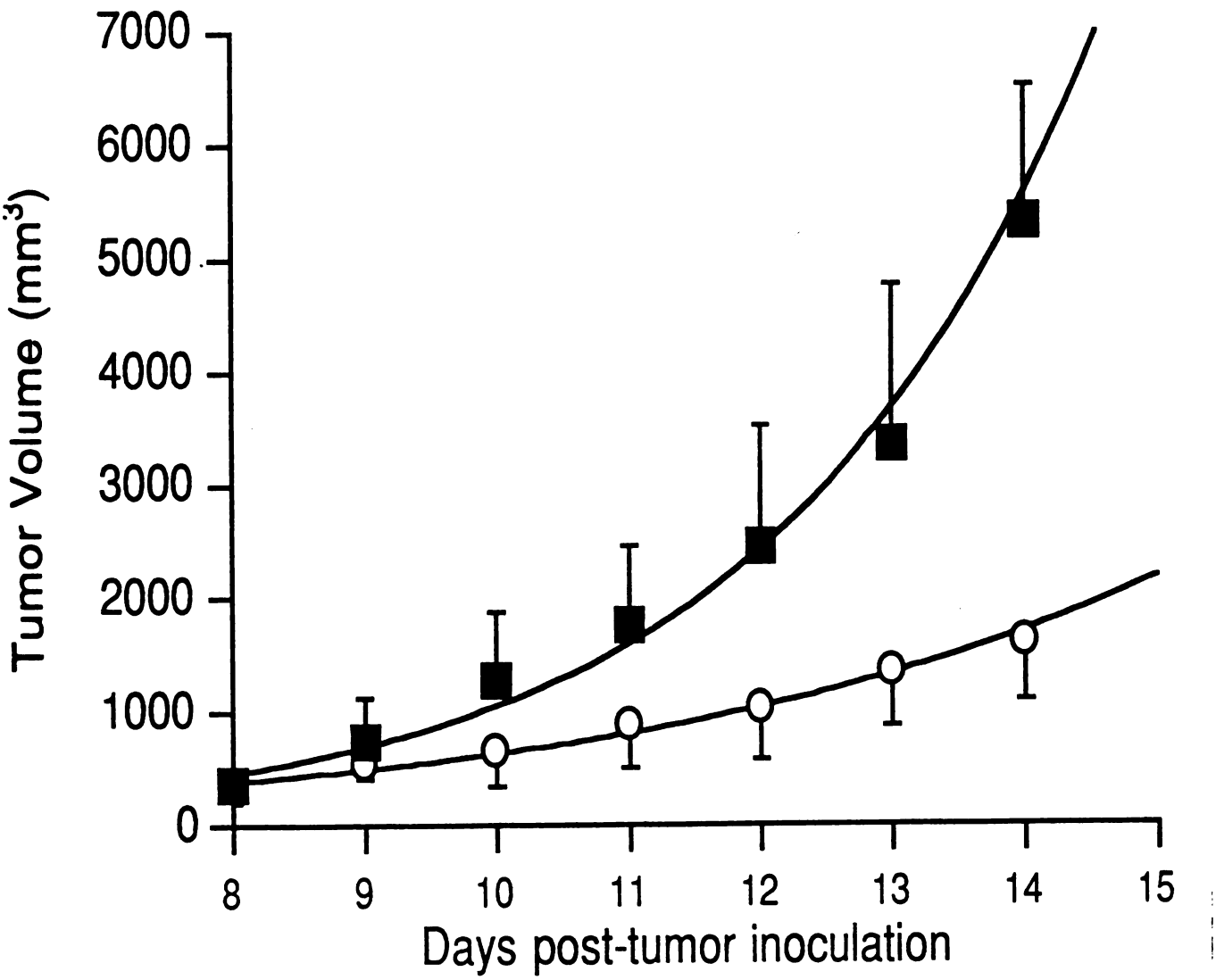

**Fig. 3** Representative SPGR (TR/TE = 50ms/1.4 ms) MR images of anti-VEGF antibody treated animal (lower row) and anti-gp120 antibody treated animal (upper row), before contrast medium (a), 1 minute (b) and 60 minutes (c) postcontrast medium administration. Based on dynamic signal intensity changes, permeability surface area product (PS) was calculated for each image element (pixel) and assigned a gray scale value to yield a pixel-by-pixel PS map (d). Arrows indicate location of implanted MDA-MB-435 breast cancers. Enhancement is noted in blood, highly vascularized liver tissue, and to a lesser degree, in the tumors. The anti-VEGF antibody treated tumor is smaller than the control treated tumor. Also note that the PS map indicates relatively reduced PS values (less intensity) in the anti-VEGF treated tumor.

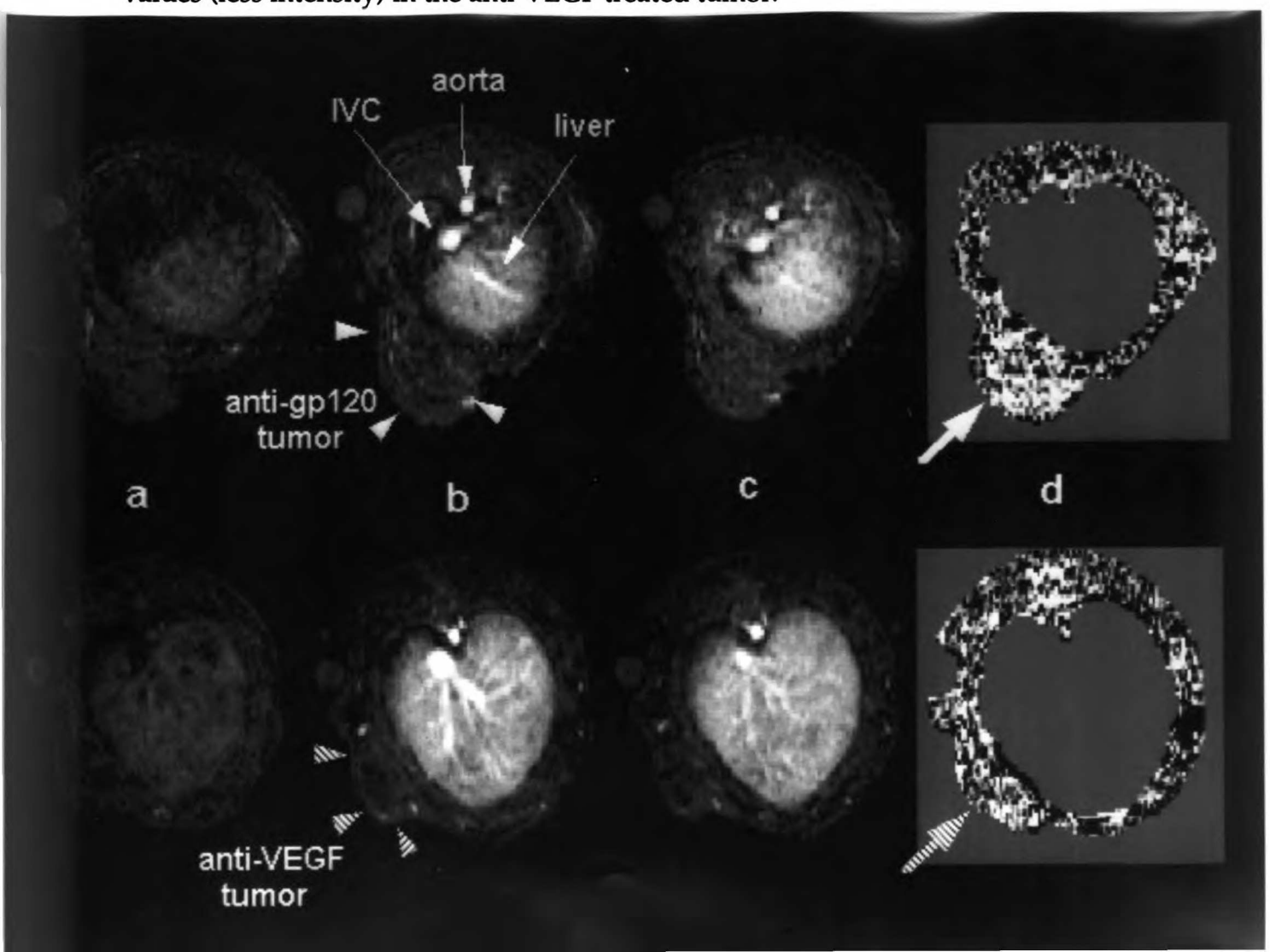

**Table 1** MRI-derived parameters of apparent microvascular permeability in breast carcinoma MDA-MB-435 of anti-gp120 and anti-VEGF treated tumors in different regions of the tumor. The data was collected from six animals in each group. Values are expressed as mean ± S.D.

* indicates statistical significance between the anti-VEGF antibody and anti-gp120 antibody treated groups ($P < 0.05$).

| **FLR ($hr^{-1}$)** | **anti-gp120** | **anti-VEGF** | **P values** |
|---|---|---|---|
| whole tumor | 0.48 ± .12 | 0.17 ± .11* | 0.03 |
| tumor rim | 0.43 ± .14 | 0.14 ± .04* | 0.009 |
| tumor center | 0.33 ± .15 | 0.13 ± .10 | 0.14 |

| **FRR ($hr^{-1}$)** | **anti-gp120** | **anti-VEGF** | **P values** |
|---|---|---|---|
| whole tumor | 0.13 ± .09 | 0.05 ± .03* | 0.039 |
| tumor rim | 0.15 ± .07 | .067 ± .04* | 0.021 |
| tumor center | 0. 09± .1 | 0.07 ± .05 | 0.41 |

**Fig. 4** Mean magnetic resonance signal response curves, indicating the changes in the relaxivity ($\Delta R_1$), of blood and tumor rim of six animals in each antibody group. The blood signal response slightly decreases over 60 minutes, whereas the tumor curves increase over the same time period. The slope of the tumor curve is approximately proportional to the microvascular permeability to macromolecular contrast agent.

($\Delta$ = blood; ■ = rim of anti-gp120 treated tumors; ○ = rim of anti-VEGF treated tumors)

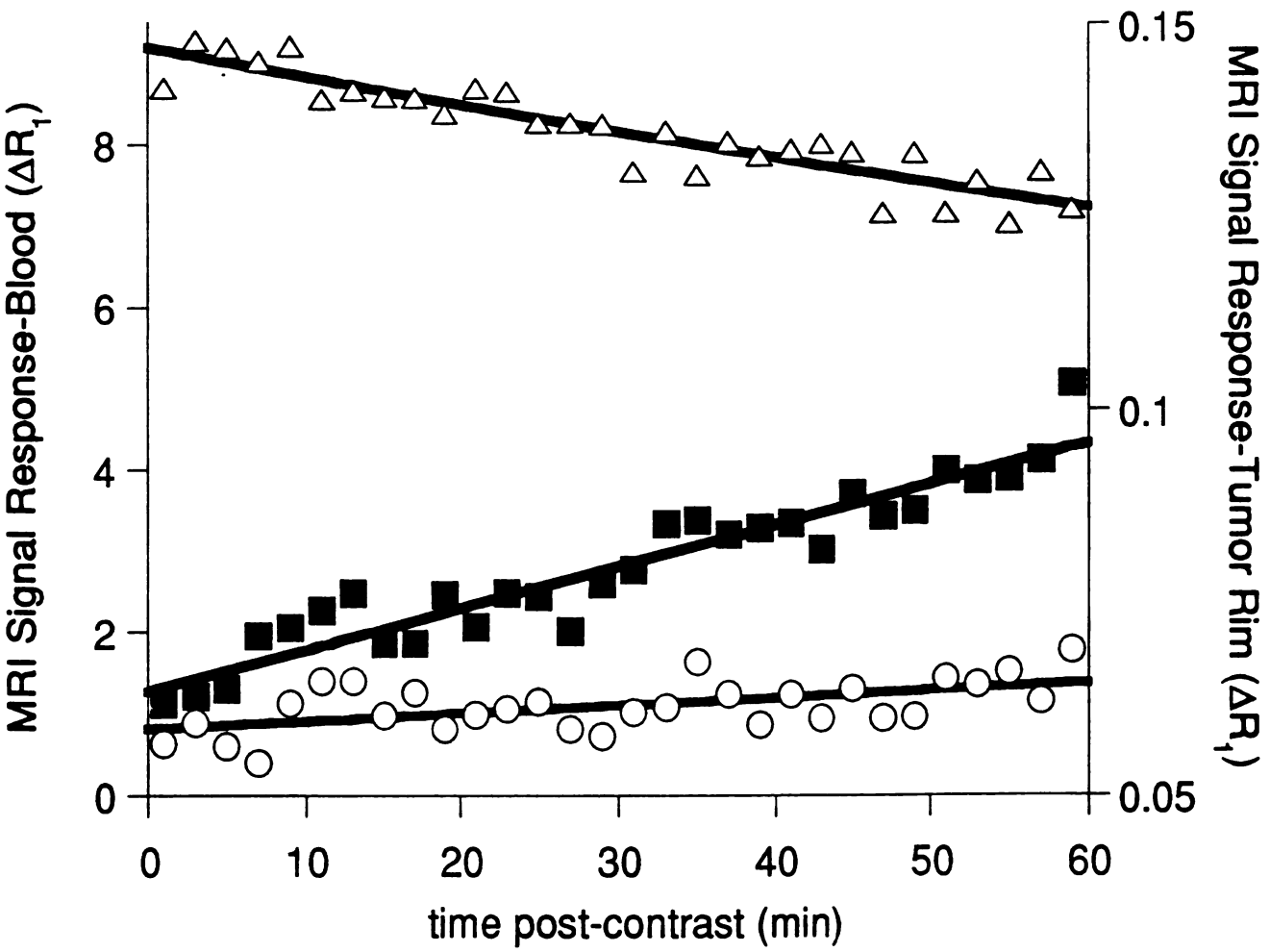

**Figure 5.** Permeability surface area product (PS) ± S.D. of anti-gp120 and anti-VEGF antibody treated tumors in different tumoral regions. Data were collected from six animals in each treatment group. Error bars represent S.D.; * indicates statistical significance of difference between the anti-VEGF antibody and anti-gp120 antibody groups ($P < 0.05$).

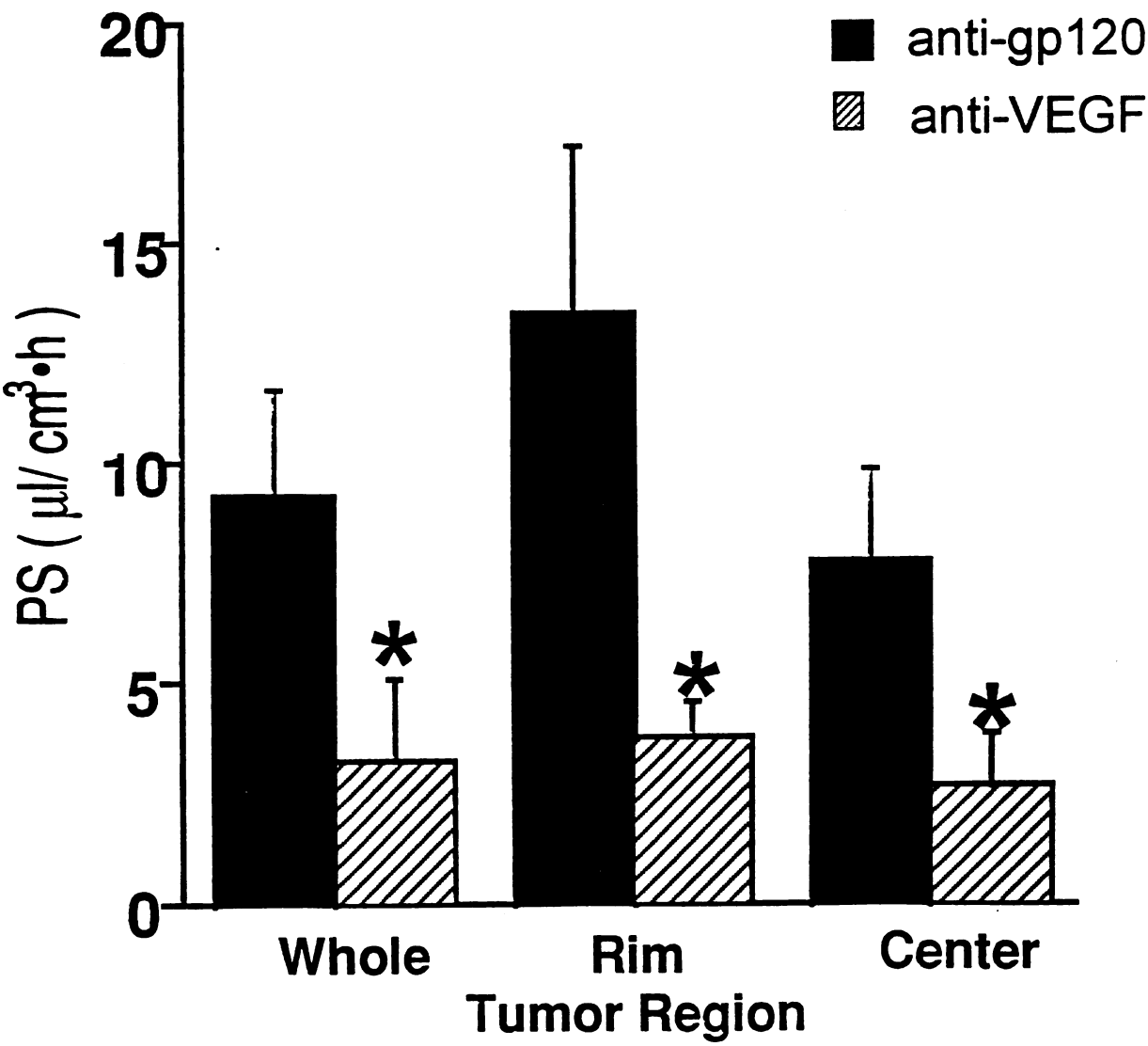

## DISCUSSION

The microvasculature of malignant tumors, as demonstrated repeatedly by invasive techniques (radiotracers, histopathology, closed circuit television) exhibit the characteristics of high density of vessels and hyperpermeability to macromolecules (34-36). These microvascular properties can be exploited by imaging assays to improve the specificity of cancer diagnosis and follow-up. The hyperpermeability of cancer microvessels is mediated, in part, by an angiogenic factor known as vascular endothelial growth factor (VEGF) (6,15-18). VEGF has been hypothesized to enhance permeability by upregulating the functional activity of vesicular-vacuolar organelles (VVO's), which have been described as endothelial cytoplasmic organelles serving as "channels" through which plasma proteins and other macromolecules can extravasate from the circulation (6,37). VEGF also promotes angiogenesis by stimulating the proliferation and migration of endothelial cells (6,9,14). The abnormally high density and hyperpermeability of microvessels can be assessed quantitatively with MMCM-enhanced MRI, as supported by the present data.

In the current study, macromolecular contrast medium-enhanced MRI defined significant reductions in the fractional leak rate (FLR) and estimated microvascular permeability surface area product (PS) in experimental human breast carcinomas following the administration of anti-VEGF antibody.

Using MMCM-enhanced MRI, mean reductions of greater than 65% in fractional leak rate and permeability surface area product were detected following administration of anti-VEGF antibody. The induced suppression of apparent tumor microvascular permeability was evident in most of the tumor regions analyzed, with the exception of FLR in the tumor center. These data are consistent with previous, although less quantitative and more invasive, studies using vital dyes to measure microvascular permeability in normal animal skin in

response to anti-VEGF antibody (12-14). By contrast, MRI provides physiological information on mammary tumors using a non-invasive imaging modality. The anti-VEGF treated tumors also demonstrated significant decreases in the growth rates and tumor weights when compared to control treated tumors. These findings are consistent with published studies (9,12,13) and confirm that anti-VEGF antibody treatment was associated with a biologically predictable response.

Tumor microvascular hyperpermeability has been hypothesized as one of the early events in the angiogenic cascade by facilitating a proteinaceous interstitial matrix favorable to the ingrowth of new capillaries ( 6,19). Hence, it is reasonable to speculate that anti-VEGF antibody may exert its anti-growth effect by blunting the enhanced permeability of tumor microvessels and inhibiting neovascularization. Alternatively, microvascular hyperpermeability could be an independent event from tumor growth. Anti-VEGF antibody treatment may directly decrease tumor growth via inhibiting neovascularization (9,12); the antibody's effect on decreasing microvascular hyperpermeability may be a coincidental observation. Because tumor growth was measured over a two-week period whereas microvascular permeability was measured at a single time point, this study was not designed to directly correlate tumor growth with microvascular permeability. To establish a correlative relationship between tumoral microvascular permeability and growth, parallel temporal measurements should be performed between these two parameters.

Data showed no significant reduction in tumor fractional blood volume following anti-VEGF antibody treatment; however, a minor trend for decreased tumor BV was observed. Perhaps a more extensive or prolonged study with additional observations would show a significant blood volume lowering effect. Alternatively, the anti-VEGF antibody treatment may prevent or limit further

microvessel formation, thus impeding tumor growth. Anti-VEGF antibody is not known to degrade pre-existing tumor microvasculature. Consequently, the relative density of microvessels, reflecting the fractional blood volume, would remain unchanged with antibody treatment.

The differences in the FLR and FRR measured in the tumor core of anti-VEGF and of anti-gp120 antibody treated tumors were not statistically significant. In some data sets, the estimates of FLR and FRR were low with large uncertainty values, which is consistent with little or no reflux of the macromolecular contrast probe from the tumor center interstitium back into the vascular compartment. As shown by Jain and coworkers , the tumor core is less vascularized, less well perfused, and experiences a greater interstitial pressure than the tumor periphery. Hence, the delivery and transendothelial transport of intravascular substrates to the tumor core is often impeded and is less predictable relative to the tumor periphery. Hence, indicators of endothelial leakiness, such as FLR and FRR, may be governed by unmeasured, often highly variable local factors such as perfusion, flow rate, interstitial pressure, stasis, and retrograde flow in the core of tumors (35). Given the multiple factors which can influence FLR and FRR and the probable small absolute reduction in endothelial leakiness in the tumor center of the anti-VEGF group, a more extensive sample providing more observations may be able to detect the reduction in these MRI-parameters. However, as with BV, there was a trend towards smaller values of FLR in the anti-VEGF treated group. Although individual parameters of BV and FLR in tumor core were not statistically reduced in the anti-VEGF antibody treated group, their product, or PS, was statistically lowered in the anti-VEGF treated group. This observation is typically seen in phenomenon that are multifactorial, such as apparent permeability in an unpredictable and often rather kinetically chaotic area such as the tumor center (34, 35). Alternately, one may consider PS a

more robust physiological parameter of apparent permeability than its individual component of FLR. PS takes into account both the supply of the macromolecular probe (BV) and its leakiness (FLR) from the vascular compartment into the tumor center interstitium.

The definition of tumor center and tumor rim was a relative anatomical distinction. Because regions-of-interests were defined in precontrast images, methodological bias of using the response (i.e. post-contrast enhancement) to define the rim and tumor center was eliminated. However, the distinction between tumor rim and center may be regarded a functional one; in contrast to the tumor core, the tumor rim is often more vascularized with more consistent pattern of vascularization and microvascular kinetics (34). In functional imaging, tumor rim may be distinguished from tumor center as the region of the tumor that experiences more rapid and brighter enhancement postcontrast (1,2,25). In the tumors studied, the anatomically defined tumor rim and center correlated well with the functional enhancement pattern of these different regions of the tumor.

Our MRI method permits the *in vivo*, non-invasive, and quantitative monitoring of tumor microvascular permeability to circulating plasma macromolecules. The imaging technique also allows complete and regional tumor sampling not available with other methods of assessing permeability. The Miles assay of dermal permeability is qualitative and cannot be easily applied to internal tissues. Imaging of radioactive tracers does not generally provide the high spatial resolution available with MRI and does not permit definition of non-target tissues on the images.

A variety of contrast-enhanced MRI and analytical techniques have been proposed for the characterization of tumors (38-41). The current technique utilizes a 3-dimensional SPGR data acquisition. This technique allows broad

anatomic multislice coverage of the entire tumor and within the central sections eliminates inflow signal aberrations for monitoring signal responses in blood. An established kinetic model of apparent permeability was employed which considers movement of contrast medium both into and out from tumor interstitium. Responses in blood signal intensity are monitored simultaneously with target tissue responses to counteract potential variations in injection rates and blood clearance, input function, and blood contrast medium concentration. Changes in the rates of longitudinal relaxation (Δ R1) were measured and applied in the kinetic analyses in preference to changes in signal intensity (ΔSI). ΔR1 is linearly related to contrast medium concentration whereas ΔSI is non-linearly related to [Gd] at all contrast medium concentrations, a potential source of significant overestimation of MRI-derived microvasculature parameters (29,31,42). Further improvements in the MRI techniques and analytical methods may provide even better accuracy of measurements.

Conclusions based on data from the present study are limited. Tumors were implanted in athymic rats which do not exhibit the usual immune responses of a human patient. MRI-derived microvascular parameters were assayed at only a single time point in tumor evolution, approximately 15 days after tumor cell inoculation. Therefore, this study did not measure the process of tumor angiogenesis as a function of its temporal evolution. Because tumor vasculature differ as a function of time and tumor size, serial measurements of tumor microvascular hyperpermeability and neovascularity using the MMCM-enhanced MRI method would be necessary to assess tumoral angiogenic response. In addition, only a single tumor type and a single contrast medium were studied. Additional studies could provide information about the time course of anti-VEGF antibody effect, the potential differences among different tumor types, and the suitability of other contrast media.

In addition, the technique cannot be immediately applied to patient studies. Although highly effective for animal experiments, albumin-(Gd-DTPA)$_{30}$, used here as a prototype macromolecular contrast medium, is not approved for clinical use. Albumin-(Gd-DTPA)$_{30}$ is incompletely eliminated from the body and thus is considered clinically unsuitable (23) Ideally, angiogenesis and tumor states could be measured using goverment-approved MRI contrast agents. However, commercially available contrast agents, which include small molecular weight iodinated compounds and gadolinium chelates, are not well designed to measure permeability. These small molecular contrast media quickly equilibrate between intravascular and extravascular spaces. It has been estimated that 10-70% of gado-pentate (excluding the CNS) diffuses from the blood into the extravascular space through the capillary endothelium (personal communication: A Muhler, Contrast Medium Research Group, Schering AG). Such rapid and heterogeneous transcapillary exchange in normal tissues limits the ability to detect or quantitate hyperpermeability associated with tumors. Thus, small molecular contrast agents provide suboptimal discrimination between normal and abnormal permeabilities as compared to macromolecular contrast agents. Carefully controlled comparisons of small molecular and macromolecular contrast media for the characterization of tumor microvascular are needed. Macromolecular contrast media with favorable pharmacokinetic properties which are being intensively developed may be available for clinical use in coming years.

Nonetheless, the current data indicate that MRI enhanced with a macromolecular contrast agent is able to detect and measure a decrease in apparent tumor microvascular permeability to macromolecules seven days after initiation of anti-VEGF antibody treatment. This technique, or a modification thereof, may prove

clinically valuable to characterize and monitor tumor microvascular characteristics, including tumor responsiveness to anti-angiogenesis drugs.

# List of Tables

Table 1

MRI-derived microvascular permeability parameters of breast carcinoma MDA-MB-435 tumors

# List of Figures

## Bibliography


1. Van Dijke C, Brasch C, Roberts T, et al. Mammary carcinoma model: correlation of macromolecular contrast enhanced MR imaging characterizations of tumor microvasculature and histologic capillary density. Radiology 1996; 198: 813-818.
2. Schwickert H, Stiskal M, Roberts T, et al. Contrast-enhanced MRI assessment of tumor capillary permeability: the effect of pre-irradiation on tumor delivery of chemotherapy. Radiology 1996; 198:893-898.
3. Folkman J. What is the evidence that tumors are angiogenesis dependent? J Natl Cancer Inst 1989; 82:4-6.
4. Folkman J. Introduction: Angiogenesis and cancer. Semin Cancer Biol 1992; 3:47-48.
5. Fidler I, Ellis L. The implications of angiogenesis for the biology and therapy of cancer metastasis. Cell 1994; 79:185-188.
6. Dvorak H, Brown L, Detmar M, et al. Vascular permeability factor/ vascular endothelial growth factor, microvascular hyperpermeability, and angiogenesis. Am. J. Path. 1995; 146:1029-1039.
7. Liotta LA, KleinerTnan J, Saidel GM. Quantitative relationships of intravascular tumor cells, tumor vessels and pulmonary metastases following tumor implantation. Cancer Research 1974; 34:997-1004.
8. Jain R, Gerlowski L. Extravascular transport in normal and tumor tissues. Crit Rev in Oncol/Hematol 1984; 5:115-170.
9. Warren, R.S., Yuan, H., Matli, M.R., Gillett, N.A., Ferrara, N. Regulation by vascular endothelial growth factor of human colon cancer tumorigenesis in a mouse model of experimental liver metastasis. *J. Clin. Invest.* 95:1789-1797, 1995.

10. Weidner N, Semple J, Welch W, Folkman J. Tumor angiogensis and metasasis- correlation in invasive breast carcinoma. N Engl J Med 1991; 324:1-8.

11. Weidner N. Intratumoral microvascular density as a prognostic factor in cancer. Am J Pathot 1995; 147:9-19.

12. Kim KJ, Li B, Winer J, et al: Inhibition of vascular endothelial growth factor-induced angiogenesis suppresses tumor growth in vivo. Nature 1993; 362:841-844.

13. Kondo S, Asano M, Suzuki H. Significance of vascular endothelial growth factor vascular pemeability factor for solid tumor growth, and its inhibition by the antibody. Biochem Biophys Res Commun 1993; 194:1234-1241.

14. Kim KJ, Li B, Houck K, et al: The vascular endothelial growth factor proteins: identification of biologically relevant regions by neutralizing monoclonal antibodies. Growth Factors 1992; 7:53-64.

15. Senger D, Van De Water, L, Brown L, et al. Vascular Permeability Factor (VPF, VEGF) in tumor biology. Cancer Metastasis Rev 1993; 12:303-324.

16. Collins P, Connolly D, Williams T. Characterization of the increase in vascular permeability induced by vascular permeability factor in vivo. Br J Pharmacol 1993; 109:195-199.

17. Nagy JA, Masse EM, Herzberg KT, Meyers MS, Yeo KT, Yeo TK, Sioussat TM, Dvorak HF. Pathogenesis of ascites tumor growth: vascular permeability factor, vascular hyperpermeability, and ascites fluid accumulation. Cancer Res. 1995; 55:360-368.

18. Dvorak, H.F., Sioussat, T.M., Brown, L.F., et al. Distribution of vascular permeability factor (vascular endothelial growth factor) in tumors: concentration in tumor blood vessels. J. Exp. Med. 1991; 174:1275-1278.

19. Nagy JA, Brown LF, Senger DR, et al: Pathogenesis of tumor stroma generation: a critical role for leaky blood vessels and fibrin deposition. Biochim. Biophys. Acta 1988; 948: 305-326.

20. Heywang-K6brunner S. Contrast-enhanced magnetic resonance imaging of the breast. Investigative Radiology 1994; 29:94-104.

21. 0. Weinreb J, Newstead G. Sate of the art: MR imaging the breast. Radiology 1995; 196:593-61 0.

22. Mkstrom MG, Moseley ME, White DL, et al. Contrast enhanced MRI of tumors: Comparison of GD-DTPA and a macromolecular agent. Investigative Radiology 1989; 24(8):609-615.

23. Schmiedl U, Ogan MD, Paajanen H, et al Albumin labeled with GD-DTPA as an intravascular, blood pool-enhancing agent for MR imaging: Biodistribution and imaging studies. Radiology 1987; 162:205-210.

24. Shames D, Kuwatsuru R, Vexier V, et al. Measurement of capillary permeability to macromolecules by dynamic magnetic resonance imaging: A quantitative non-invasive technique. Magnetic Resonance in Medicine 1993; 29:616-622.

25. Cohen F, Kuwatsuru R, Shames D, et al. Contrast enhanced MRI estimation of altered capillary permeability in experimental mammary carcinomas following x-irradiation. Invest Radiol 1995; 29:970-977.

26. Kuwatsuru R, Shames D, Mohler A, et al. Quantification of tissue plasma volume in the rat by contrast-enhanced magnetic resonance imaging. Mag Res Med 1993; 30:76-81.

27. Price JE, Polyzos A, Zhang RD, et al: Tumorigenicity and metastasis of human breast carcinoma cell lines in nude mice. Cancer Res. 1990; 50:717-721.

28. Ingber D, Fujita T, Kishimoto S, et al: Synthetic analogues of fumagilin that inhibit angiogenesis and suppress tumor growth. Nature 1990; 348: 555-557.

29. Schwickert HC Roberts TPL, Shames DM, et al: Quantification of liver blood volume: comparison of ultra short T1 inversion recovery echoplanar imaging (ULSTIR-EPI), with dynamic 3D-gradient recalled echo imaging. Mag Reson Med. 1995; 34:845-852.

30. Ogan MD, Schmiedl U, Moseley ME, et al: Albumin labeled with Gd-DTPA-an intravascular contrast-enhancing agent for magnetic resonance blood pool imaging: preparation and characterization. Invest. Radiol. 1987; 22: 665-671.

31. Schwarzbauer C, Syha J, Haase A. Quantification of regional blood volumes by rapid Tl mapping. Mag Reson Med 1993; 29:709-712.

32. Renkin EM. Transport of potassium-42 from blood to tissue in isolated mammalian skeletal muscles. Am J Physiol 1959; 197:1205-1210.

33. Crone C. The permeability of capillaries invarious organs determined by the use of the "indicator diffusion" method. Acta Physiol Scand 1963; 58:292-305.

34. Jain R. Transport of molecules in the tumor interstitium: a review. Cancer Res. 1987; 47: 3039-3051.

35. Jain R. Transport of molecules across tumor vasculature. Cancer and Metastasis Reviews 1987; 6:559-593.

36. Heuser L, Miller F. Differential macromolecular leakage from the vasculature of tumors. Cancer 1986; 57:461-464.

37. Kohn S, Nagy J, Dvorak H, et al. Pathways of macromolecular tracer transport across venules and small veins, structural basis for the hyperpermeability of tumor blood vessels. Lab Invest 1992; 76:596-607.

38. Buadu L, Murakami J, Murayama S, et al. Correlation between contrast-enhanced MR imaging of the breast and tumor angiogenesis: a quantitative and qualitative study. In: Annual Meeting American Roentgen Ray Society. 1996. San Diego, CA. 58.

39. Stack JP, Redmond OM, Codd MB, et al. Breast disease: tissue characterization with GD-DTPA enhancement profiles. .Radiology 1990; 174:4914.

40. Spraggins T, de Paredes E, DeAngelis G. Three-dimensional keyhole imaging: application to dynamic contrast-enhanced MRI of the breast. In: Proceedings of the Society of Magnetic Resonance in Medicine. 1993. Berkeley, CA. 11 8.

41. Stomper P, Her-man S, Klippenstein D, et al Suspect breast lesions: findings at dynamic gadolinium-enhanced MR imaging correlated with mammographic and pathologic features. Radiology 1995; 197:3 87-395

42. Donahue KM, Burstein D. Relaxivity of GD-DTPA in tissue. In: 11th Annual Meeting of Soc Magn Reson Med. 1992. Berlin, Germany. 1330.

## Acknowledgments

This research was partially supported by the Breast Cancer Fund of the State of California through the Breast Cancer Program of the University of California, Grant number 1RB-0139; and by the developmental grant from the UCSF SPORE, CA 58207.

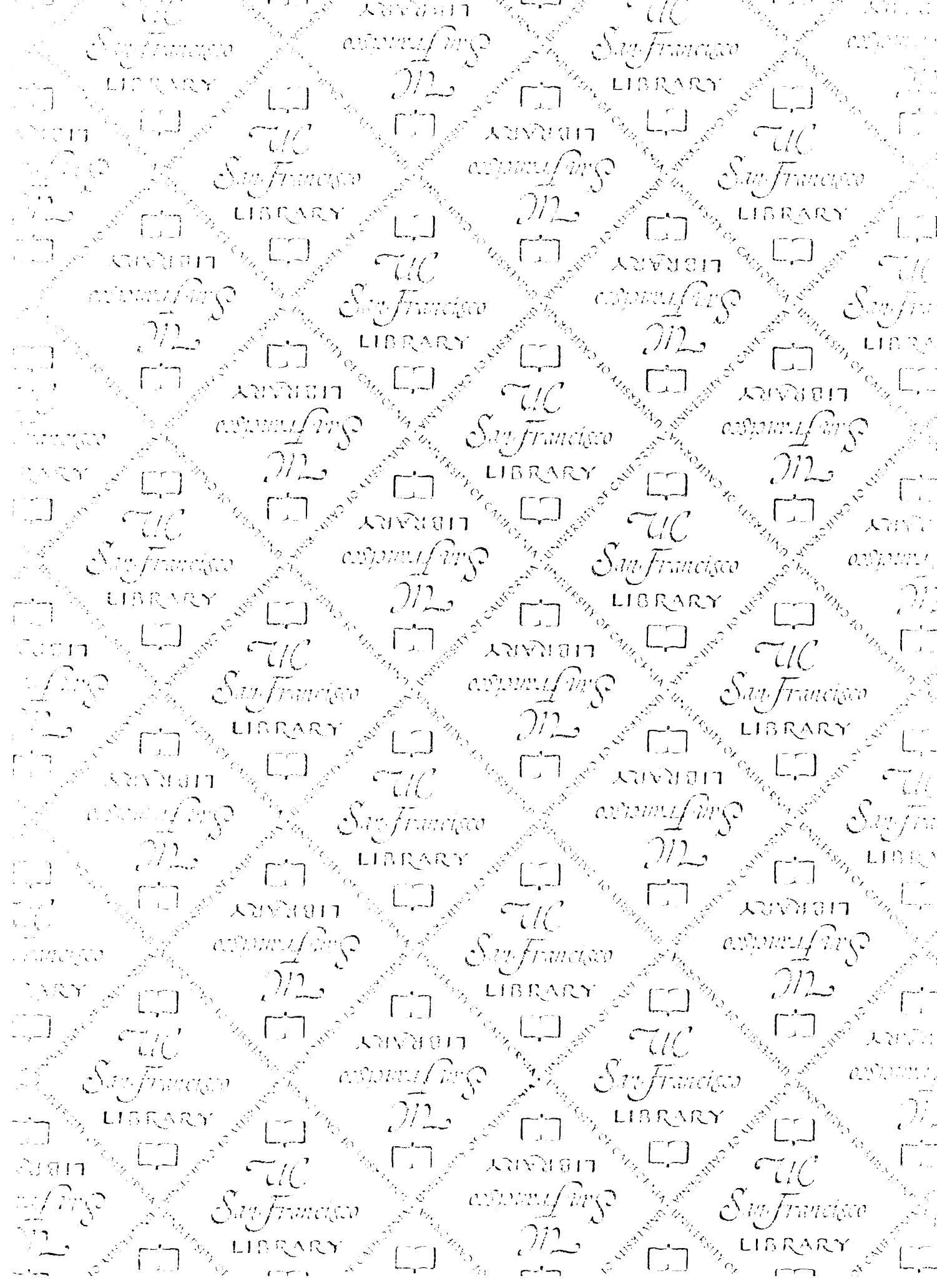
UC
San Francisco
LIBRARY